Journal of Materials Chemistry A

REVIEW

View Article Online
View Journal | View Issue

Cite this: J. Mater. Chem. A, 2015, 3, 8970

Review of recent progress in chemical stability of perovskite solar cells

Guangda Niu, Xudong Guo and Liduo Wang*

In recent years, the record efficiency of perovskite solar cells (PSCs) has been updated from 9.7% to 20.1%. However, there has been very little study of the issue of stability, which restricts the outdoor application of PSCs. The issues of the degradation of perovskite and the stability of PSC devices should be urgently addressed to achieve good reproducibility and long lifetimes for PSCs with high conversion efficiency. Without studies on stability, exciting achievements cannot be transferred from the laboratory to industry and outdoor applications. In order to improve their stability, a basic understanding of the degradation process of PSCs in different conditions should be acquired *via* thorough study. This review summarizes recent studies of the relationship of the chemical stability of PSCs with their environment (oxygen and moisture, UV light, solution process, temperature) and corresponding possible solutions.

Received 21st September 2014
Accepted 2nd December 2014

DOI: 10.1039/c4ta04994b

www.rsc.org/MaterialsA

1. Introduction

The class of inorganic–organic hybrid compounds ($CH_3NH_3PbX_3$, X = I, Br, Cl), with the crystal structure of perovskite, have emerged as brilliant light absorbers in solar cells. These ambipolar semiconductors have attracted increasing attention due to their easy fabrication process, small band-gaps, high extinction coefficients, and high carrier mobility.[1–3] The thin film solar cells based on these materials are termed perovskite solar cells (PSCs).

During the past several years, research into PSCs has increased. The editors of Science selected PSCs as a runner-up for the Top 10 Breakthroughs of 2013.[4] The first report of a PSC incorporating methylammonium lead iodide was demonstrated by Miyasaka and co-workers in 2009. They employed $CH_3NH_3PbI_3$ and the analogue $CH_3NH_3PbBr_3$ as sensitizers in liquid-electrolyte-based dye-sensitized solar cells.[5] However, the liquid electrolytes in their work, which were iodine redox, dramatically corroded the perovskite and led to a low power conversion efficiency (PCE) of only 3.81%. In 2012, the introduction of the organic hole-transport material spiro-OMeTAD, replacing liquid electrolytes, improved the stability of perovskite in the devices significantly and achieved an unexpected PCE of up to 9.7%.[6] Then, numerous researchers entered this field, leading to many exciting experimental results, including the underlying mechanism responsible for the unusually high conversion efficiency, various fabrication methods for the perovskite films, and an increase in the record efficiency from 9.7% to 20.1% in only two years.[7–9] It should be noted that Snaith and co-workers thoroughly studied meso-superstructured solar cells (MSSCs), which

Key Lab of Organic Optoelectronics and Molecular Engineering of Ministry of Education Department of Chemistry, Tsinghua University, Beijing 100084, China. E-mail: chldwang@mail.tsinghua.edu.cn

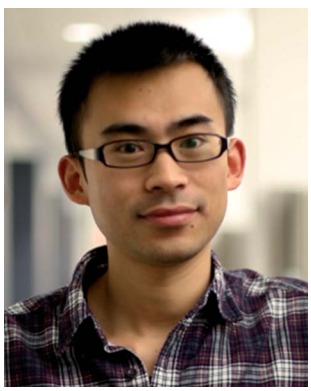

Guangda Niu was born in Hebei, China, in 1988. He received a BS degree in Chemistry (2011) from Nanjing University. Since then, he has been pursuing his PhD degree at Tsinghua University under the supervision of Prof. Liduo Wang. His research interests include the rational design of inorganic–organic hybrid perovskite solar cells, quantum dot sensitized solar cells, and the application of metal nanomaterials in solar cells.

Xudong Guo was born in Henan, China, in 1990. He received a BS degree in Chemistry (2012) from Tsinghua University. Currently, he is pursuing his MS degree at Tsinghua University under the supervision of Prof. Liduo Wang. His research interests include inorganic–organic hybrid perovskite solar cells and dye sensitized solar cells.

employ mesoporous alumina as an inert scaffold to support the perovskite.[10] In MSSCs, spiro-OMeTAD, perovskite, and a thin TiO_2 layer form the p–i–n junction, which is different from that of sensitized solar cells, resulting in considerably lower processing temperatures and improved cell stability. Additionally, many other groups have also fabricated solar cells with perovskite as absorbers, but without hole-transport materials, which have also shown brilliant efficiency.[11,12] The heterojunction between $CH_3NH_3PbI_3$ and TiO_2 is responsible for the charge separation. Moreover, in order to construct planar perovskite thin films, several fabrication routes have been developed, including the solution processable method (spin-coating), vacuum evaporation process, and vapor-assisted solution process.[8,10,13] According to the latest chart of record cell efficiencies from the National Renewable Energy Laboratory (NREL), the highest confirmed record PCE is 20.1%, by researchers from the Korean Research Institute of Chemical Technology.[14] Yang and co-workers very recently reported that they have achieved an efficiency of 19.3% in a planar geometry.[9]

Currently, there are two key issues for the application of PSCs in industry: power conversion efficiency and device stability. As previously illustrated, the present research on PSCs mainly focuses on high performance *via* different device structures, fabrication methods, and various analogues. Based on the rapid progress in this field, several reviews or feature articles have thoroughly described the emergence of perovskites in solar cells, future directions to improve efficiencies, and recent developments in perovskite solar cells such as materials design, novel cell structures, and underlying mechanisms.[15–17] However, the stability of PSCs, which restricts their outdoor photovoltaic applications, is often ignored in studies. The issues of the degradation of perovskite and the stability of the devices should be urgently addressed to achieve good reproducibility and a long lifetime for PSCs with high conversion efficiency. Without studying the stability, we cannot transfer these exciting achievements from the laboratory to industry and outdoor applications.

Liduo Wang is a professor of the Department of Chemistry in Tsinghua University. He received his PhD degree in Nagoya University of Japan in 1995. Dr Wang has once worked as a visiting scholar in the Department of Chemistry and as the research associate in the Department of Electrical and Electronic Engineering in The Hong Kong University of Science and Technology, and as a postdoctoral researcher in Department of Materials Science and Engineering, Tsinghua University. His current research interests include perovskite solar cells, organic–inorganic semiconductor multilayer, and its optoelectronic properties.

The chemical stability of PSCs, which refers to a series of chemical reactions of the perovskite films under different atmospheres and conditions, is the major factor affecting the stability of PSCs. Methylammonium lead iodide can be taken as an example to illustrate the chemical stability of perovskite. The following chemical equation should be always taken into consideration:

$$PbI_2\ (s) + CH_3NH_3I\ (aq) \leftrightarrow CH_3NH_3PbI_3\ (s) \quad (1)$$

The positive direction is the synthetic process of methylammonium lead iodide and the negative direction is the decomposition process of the perovskite. All other types of perovskite, such as $CH_3NH_3PbBr_3$ and $CH_3NH_3PbI_2Cl$, undergo similar reactions, simply replacing the reactants with the corresponding chemicals.

Generally speaking, there are two major routes for the decomposition of $CH_3NH_3PbI_3$. First, if PbI_2 and/or CH_3NH_3I combines with other components, then the chemical equilibrium can drive reaction (1) in the negative direction, leading to the decomposition of perovskite in the films and thus decreasing the chemical stability of the PSCs. Second, the perovskite in the film can directly degrade into other chemicals under certain conditions.

The synergy of degradation by the materials themselves under different environmental conditions leads to different problems that affect the chemical stability of PSCs. Typically, PSCs are susceptible to the following four factors: oxygen and moisture, UV light, the solution process (solvents, solutes, additives), and temperature. This review mainly focuses on the recent studies regarding the relationship of the chemical stability of PSCs with the aforementioned factors and the corresponding possible solutions, combined with our own understanding of the stability of PSCs. The aim is to provide a better understanding of the most important factors that should be taken into consideration in outdoor applications, and how to control the stability of PSCs in different conditions.

2. Chemical stability of PSCs under different environmental conditions

2.1 The chemical stability of PSCs in oxygen and moisture

During the process of assembling and testing, oxygen and moisture in the atmosphere can directly affect the stability of the components in reaction (1). First, due to the high sensitivity of $CH_3NH_3PbI_3$ to water, it tends to hydrolyze in the presence of moisture, leading to the degradation of perovskite, which occurs as follows:

$$CH_3NH_3PbI_3\ (s) \leftrightarrow PbI_2\ (s) + CH_3NH_3I\ (aq) \quad (2a)$$

$$CH_3NH_3I\ (aq) \leftrightarrow CH_3NH_2\ (aq) + HI\ (aq) \quad (2b)$$

$$4HI\ (aq) + O_2\ (g) \leftrightarrow 2I_2\ (s) + 2H_2O\ (l) \quad (2c)$$

$$2HI\ (aq) \leftrightarrow H_2\ (g) + I_2\ (s) \quad (2d)$$

It should be noted that moisture, oxygen, and UV radiation are indispensable for the degradation process. Additionally, the equilibrium of reaction (2b) leads to the co-existence of CH_3NH_3I, CH_3NH_2, and HI in the film. There are two methods for HI to degrade in the next step. One method is a redox reaction in the presence of oxygen (2c); the other method is a photochemical reaction, in which HI can decompose into H_2 and I_2 under UV radiation (2d). The consumption of HI, according to reactions (2c) and (2d), drives the whole degradation process forward.

As the degradation of organic–inorganic halide perovskite is quite sensitive to moisture and oxygen, most of the fabrication process must be conducted in a glove box filled with inert gas.[8,10] However, when the assembled devices are measured under ambient conditions, significant degradation of the organic–inorganic halide perovskite is typically observed. Seok and co-workers reported that $CH_3NH_3PbI_3$ started to decompose at a humidity of 55%, which could be observed by a remarkable color change from dark brown to yellow.[18] The degradation of perovskite led to an unwanted decrease in efficiency, which restricts the outdoor applications of PSCs. Several researchers have studied how moisture and oxygen affect the stability of perovskite solar cells.

Our previous work verified that oxygen, together with moisture, could lead to the irreversible degradation of $CH_3NH_3PbI_3$ according to reactions (2a–d).[19] The absorption of $TiO_2/CH_3NH_3PbI_3$ film between 530 nm and 800 nm greatly decreased after exposure to air with a humidity of 60% at 35 °C for 18 h (Fig. 1a). XRD spectra revealed that the original peaks of $CH_3NH_3PbI_3$ all disappeared (Fig. 1b), implying the complete degradation of $CH_3NH_3PbI_3$. The new peaks located at 34.3, 39.5, and 52.4° after degradation are attributed to the (102), (110), and (004) planes of hexagonal 2H polytype PbI_2, and another new peak at 38.7° is assigned to the (201) plane of orthorhombic I_2.

The color change of CH_3NH_3I under different conditions demonstrated that only air and UV radiation could lead to the brown color, which is due to the existence of I_2 (inset in Fig. 1a). An amorphous Al_2O_3 layer has been used as a representative modification material in dye sensitized solar cells and liquid state perovskite solar cells.[20,21] We found that Al_2O_3 could also protect perovskite from degradation in solid-state PSCs, and the devices modified with Al_2O_3 showed better stability than those without modification.

Another study from Walsh and co-workers proposed a similar decomposition pathway for $CH_3NH_3PbI_3$ in the presence of water.[22] First, a single water molecule, which is a Lewis base, combines with $CH_3NH_3PbI_3$ and removes one proton from ammonium, leading to the formation of the intermediates $[(CH_3NH_3^+)_{n-1}(CH_3NH_2)PbI_3][H_3O^+]$. Then, the intermediates can decompose into HI, CH_3NH_2, and finally into PbI_2 by phase changes of hydrogen iodide (soluble in water) and methylammonium (volatile and soluble in water). Based on the proposed reaction mechanism, it was believed that a hybrid perovskite incorporating aprotic organic ions, such as tetramethylammonium, $(CH_3)_4N^+$, which could not provide protons from the ammonium, might be chemically stable in the presence of water.

Some researchers found that $CH_3NH_3PbI_3$ is more sensitive to moisture than $CH_3NH_3PbBr_3$. However, the absorption of pure $CH_3NH_3PbBr_3$ is not comparable to that of $CH_3NH_3PbI_3$.[23,24] Therefore, Seok and co-workers studied the employment of chemically tuned $CH_3NH_3Pb(I_{1-x}Br_x)_3$ as sensitizers in PSCs.[18] Interestingly, the devices with $CH_3NH_3Pb(I_{1-x}Br_x)_3$ (x = 0.2, 0.29) exhibited good stability after exposure to 55% humidity for 20 days, as well as high power conversion efficiency. This may be due to a structure phase transfer from the tetragonal phase into the cubic phase, caused by the substitution of larger iodide atoms with smaller bromide atoms.

Additionally, Karunadasa and co-workers recently employed two-dimensional (2D) hybrid perovskites, $(PEA)_2(MA)_2[Pb_3I_{10}]$ ($PEA = C_6H_5(CH_2)_2NH_3^+$, $MA = CH_3NH_3^+$), as absorbers in PSCs.[25] The high-quality films obtained through spin coating under ambient conditions, without annealing, are more resistant to moisture than that using $(MA)[PbI_3]$ (Fig. 2a). Powder

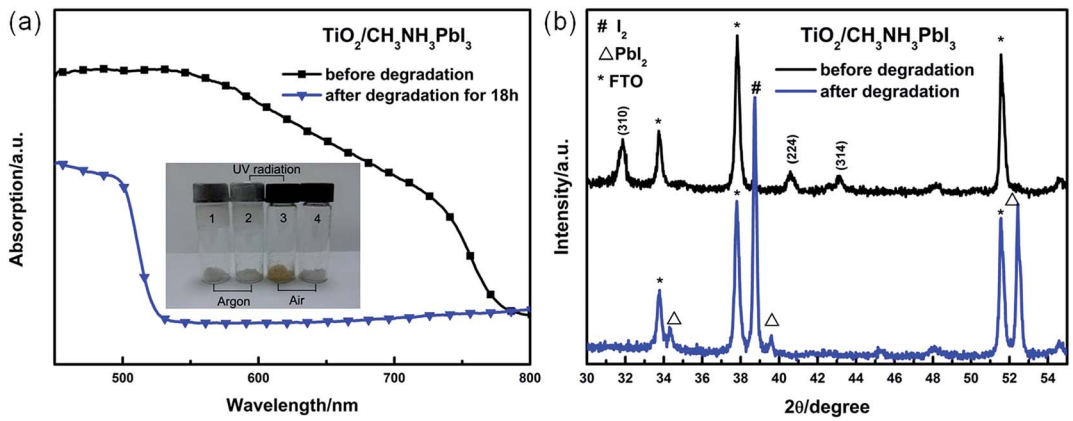

Fig. 1 Degradation of $CH_3NH_3PbI_3$ in moisture and air atmosphere. (a) UV-vis absorption spectra of $TiO_2/CH_3NH_3PbI_3$ film before and after degradation. The inset is a photograph of CH_3NH_3I exposed to different conditions: (1) CH_3NH_3I exposed to argon and without UV radiation. (2) CH_3NH_3I exposed to argon and with UV radiation. (3) CH_3NH_3I exposed to air and with UV radiation. (4) CH_3NH_3I exposed to air and without UV radiation. (b) XRD patterns of $TiO_2/CH_3NH_3PbI_3$ film before and after degradation. Adapted from ref. 19 with permission from The Royal Society of Chemistry.

X-ray diffraction (PXRD) patterns illustrate that after exposure to a humidity level of 52% for 46 days, the crystal structure of $(PEA)_2(MA)_2[Pb_3I_{10}]$ was retained, but $(MA)[PbI_3]$ completely degraded into PbI_2. The stability of $(PEA)_2(MA)_2[Pb_3I_{10}]$ in moisture benefits from its 2D layer structure, as shown in Fig. 2b. The layered structure was derived from $(MA)[PbI_3]$ by slicing along specific crystallographic planes. PEA was inserted between two inorganic layers, which were comprised of three sheets of corner-sharing metal-halide octahedra in each layer. Previous reports stated that when the inorganic layers were comprised of one or two sheets of octahedral metal-halides, the exciton binding energy was too high, leading to strongly bound excitons with low mobility.[26,27] However, $(PEA)_2(MA)_2[Pb_3I_{10}]$ exhibits similar exciton binding energy (*circa* 40 meV) compared to $(MA)[PbI_3]$, which is beneficial for the fabricated solar cells.

Moreover, some effective encapsulation methods for CIGS cells could be employed to improve the stability of perovskite solar cells. For example, double glass layers have been successfully applied in commercial CIGS modules to prevent moisture penetration.[28] These techniques could also work in perovskite solar cells.

Most recently, Yang and co-workers discovered a significant phenomenon: when they fabricated perovskite solar cells in controlled humidity conditions, the power conversion efficiency was boosted to a maximum of 19.3% in a planar geometry.[9] They proposed a reconstruction mechanism induced by moisture. The hygroscopic organic species could be dissolved by moisture; thus, the transport of chemicals in the film would be accelerated. Three stages of the phase transformation of perovskite from PbI_2 to a mixture of $CH_3NH_3PbI_3$ and $CH_3NH_3PbCl_3$, and finally to $CH_3NH_3PbI_3$ and/or $CH_3NH_3PbI_{3-x}Cl_x$, were verified from the XRD and SEM results. However, after the devices were fabricated, they still suffered the effects of moisture. The power conversion efficiency retained less than 5% of the original performance after 6 days of storage in ambient atmosphere.

2.2 The chemical stability of PSCs in UV light

In PSCs, the most commonly used photoanodes are composed of compact or mesoporous TiO_2. However, titanium oxide, which has a band-gap of 3.20 eV, is a typical photocatalyst for oxidizing water to create hydroxyl radicals, and for oxidizing organic materials.[29] When used as a photoanode in dye-sensitized solar cells, it can extract electrons from iodide (I^-) in the electrolytes. Hitoshi and co-workers found that after light exposure for 12 h, the original $CH_3NH_3PbI_3$ layer was transformed into PbI_2, as evidenced by the decreased UV-vis absorption and XRD patterns.[30] They proposed a possible mechanism to explain the degradation process in the film under light exposure as follows:

$$2I^- \leftrightarrow I_2 + 2e^- \text{ [at the interface between } TiO_2 \text{ and } CH_3NH_3PbI_3] \quad (3a)$$

$$3CH_3NH_3^+ \leftrightarrow 3CH_3NH_2 \uparrow + 3H^+ \quad (3b)$$

$$I^- + I_2 + 3H^+ + 2e^- \leftrightarrow 3HI \uparrow \quad (3c)$$

First, TiO_2 extracts electrons from I^- and deconstructs the structure of the perovskite, leading to the formation of I_2 (3a). Then, although the pK_a of the equation ($CH_3NH_3^+ + H_2O \leftrightarrow CH_3NH_2 + H_3O^+$) is 10.80,[31] suggesting that the equilibrium should be shifted to the left side, the continuous elimination of H^+ through reaction (3c) and evaporation of CH_3NH_2 (b.p. 17 °C) drives the reaction (3b) forward. Finally, extracted electrons at the interface between TiO_2 and $CH_3NH_3PbI_3$ can return to reduce I_2, and the formed HI can easily evaporate due to its low boiling point (Fig. 3a). In order to improve the stability of the perovskite under light exposure, Sb_2S_3 was inserted at the interface between mp-TiO_2 and $CH_3NH_3PbI_3$. They noticed that with the Sb_2S_3 surface blocking layer, the stability of the perovskite layer under light exposure was significantly enhanced, and the perovskite crystal structure

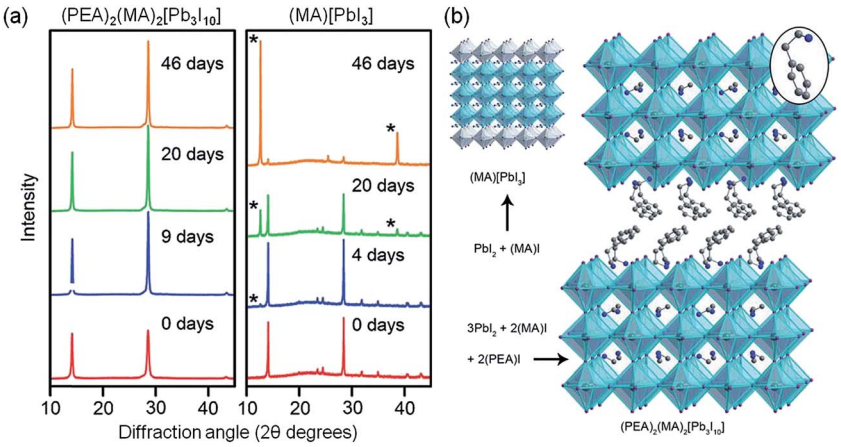

Fig. 2 (a) PXRD patterns of $(PEA)_2(MA)_2[Pb_3I_{10}]$ and $(MA)[PbI_3]$ films exposed to 52% relative humidity for certain time periods. For the $(MA)[PbI_3]$ films, annealing was conducted for 15 minutes at 100 °C prior to humidity exposure. The asterisks represent reflections from PbI_2. (b) Crystal structures of 3D perovskite (MA)[PbI3] and 2D perovskite $(PEA)_2(MA)_2[Pb_3I_{10}]$. The 2D perovskite was derived from the 3D perovskite by slicing along specific crystallographic planes. The inset shows a PEA cation in the organic layers. Atom colors: Pb = turquoise, I = purple, N = blue, C = gray. Adapted with permission from ref. 25, Copyright© 2014 WILEY-VCH Verlag GmbH & Co. KGaA, Weinheim.

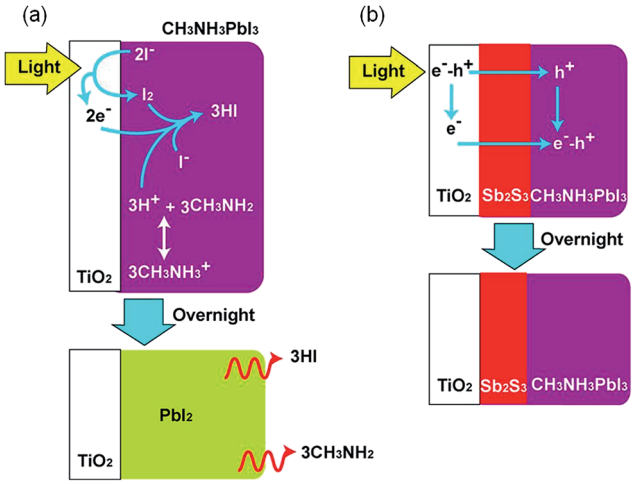

Fig. 3 Degradation scheme of $CH_3NH_3PbI_3$ during UV light exposure tests (a) without SbS modification layer, (b) with SbS modification layer. Reprinted with permission from ref. 30. Copyright 2014 American Chemical Society.

and the wavelength edges of the absorption were retained. This stability enhancement was attributed to the blocking effect of the Sb_2S_3 layer, which could deactivate the reaction of I^-/I_2 at the surface of TiO_2, as shown in Fig. 3b.

Snaith and co-workers studied the stability of PSCs under UV radiation for the first time.[32] They found that after encapsulation in a nitrogen atmosphere, perovskite solar cells with TiO_2 as the photoanode suffered from a rapid decay in photocurrent and power conversion efficiency.[32,33] The non-encapsulated devices exhibited considerably better stability. They suggested that oxygen is necessary for these devices, because it could remove the surface states of TiO_2, as shown in Fig. 4. As a typical n-type semiconductor, many oxygen vacancies are located at the surface of TiO_2 particles.[34] These electron-donating sites can combine with oxygen, which adsorbs to the oxygen vacancy sites (Fig. 4a). After UV illumination, an electron–hole pair forms on TiO_2 and the hole in the valence band combines with the electron at the oxygen adsorption site. Then, the desorption of oxygen from the sites occurs (Fig. 4b). The remaining unoccupied sites serve as trap states, which can bind with photo-induced electrons from sensitizers (Fig. 4c). Finally, the immobile trapped electrons recombine with the holes on the hole-transporting materials (Fig. 4d). The presence of oxygen could decrease the number of empty deep trap sites because they could adsorb on TiO_2 to pacify these sites. Al_2O_3 has been shown to be a promising scaffold to replace n-type TiO_2. When Al_2O_3 is used as an insulating layer in meso-superstructured solar cells (MSSC), the devices display stable performance for a period of over 1000 h.[32] Moreover, the deterioration of the devices can be inhibited by introducing an insulating alumino-silicate shell around the TiO_2 nanoparticles.[33]

Another route to prevent UV degradation is to prevent the TiO_2 from absorbing UV light by adding a UV filter in front of the TiO_2. Komarala and co-workers fabricated PSCs coated with a down-shifting (DS) $YVO_4:Eu^{3+}$ nano-phosphor layer.[35] Due to its specific 4f electronic structure,[36] europium (Eu^{3+}) doped yttrium vanadate (YVO_4) absorbs UV light and emits visible light, which could be absorbed by the perovskite layer. After spray coating the nano-phosphor layer on the reverse side of fluorine doped tin oxide (FTO) glass, as shown in Fig. 5, the device showed an improvement in stability under prolonged illumination, retaining more than 50% of its initial efficiency, whereas for PSCs without the phosphor layer, the efficiency degraded to 35% of its initial value. Additionally, a ~8.5% enhancement in photocurrent could be achieved due to the down-shifting of UV photons into additional red photons.

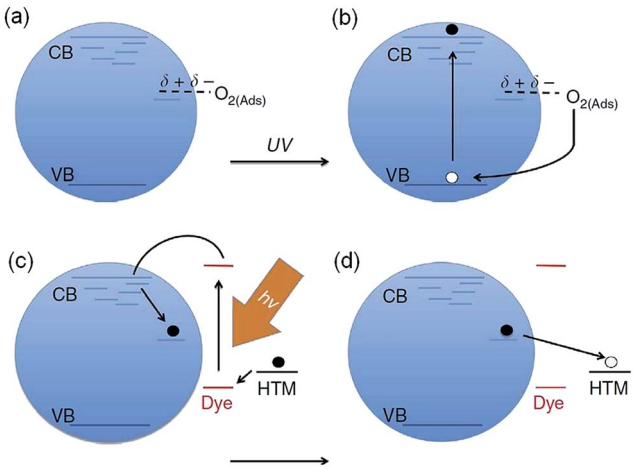

Fig. 4 Mechanism illustration of the impact of oxygen on TiO_2 nanocrystals. Adapted with permission from ref. 32, Copyright© 2013 Nature Publishing Group.

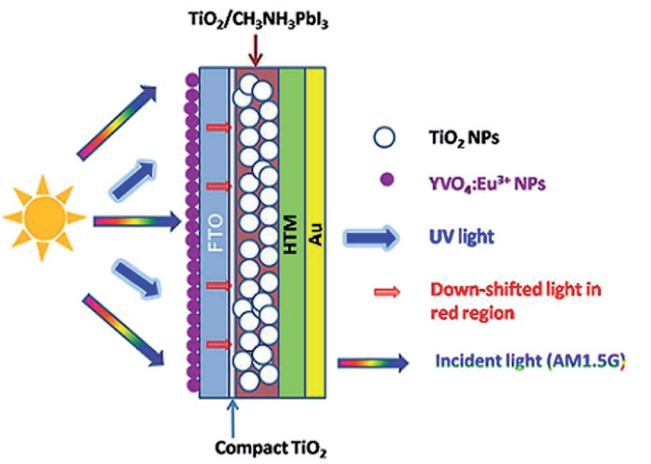

Fig. 5 Perovskite solar cell structure with down-shifting nano-phosphor layer spray coated on the reverse side of FTO glass. Reprinted with permission from ref. 35. Copyright 2014, AIP Publishing LLC.

2.3 The chemical stability of PSCs in the solution process

Different methods have been developed for perovskite film construction, such as solution processes, vapor deposition processes, and vapor-assisted solution processes. Compared to the vapor deposition process, the solution process provides simple and easy procedures, low cost, and adjustable components in the films. Therefore, most recent research has been focusing on the development of solution processes for perovskite fabrication.

During the solution preparation, for both mesoporous structure and planar structure, components from the solvents, solutes, additives or impurities may destroy the crystal structure of the perovskite. For example, our previous research found that 4-*tert*-butylpyridine (TBP), a typical additive in the hole transport layer (HTL), can dramatically influence the chemical stability of perovskite, which will be illustrated in detail later.[37] In order to avoid the use of TBP, Ma and co-workers used ionic liquid *N*-butyl-*N*′-(4-pyridylheptyl) imidazolium bis(trifluoromethane) sulfonamide (BuPyIm-TFSI) as the replacement. BuPyIm-TFSI improved the conductivity of HTL and reduced the dark current of the solar cells.[38] The commonly used HTL additives, Li-TFSI (Li-bis(trifluoromethanesulfonyl) imide) and TBP, could improve the conductivity for both triphenylamine hole transport materials such as spiro-MeOTAD, and thiophene HTMs such as P3HT.[39] However, acetonitrile, which is the solvent used with Li-TFSI, can also corrode perovskite, leading to the discarding of acetonitrile in the HTL.[8,10,13,40,41] Consequently, considerably more attention should be paid to the chemical stability of perovskite during the solution process.

The corrosion of perovskite by TBP was evidenced by a rapid decrease in the absorption intensity of the TiO_2/perovskite film upon the dropping of TBP on the film, resulting in the faded color of the film (Fig. 6). $CH_3NH_3PbI_3$ was decomposed by the dissolution of PbI_2 in TBP. The XPS results proved that TBP could react with PbI_2, forming [$PbI_2 \cdot x$TBP] complexes. When assembled in PSCs, TBP in the HTM could make contact with the perovskite layer and influence the stability. However, TBP is indispensable in HTM because it can effectively suppress the electron recombination process from TiO_2 to the electrolytes, as well as improve the contact between perovskite and the HTL by increasing the polarity of the HTL. In the presence of TBP, the open-circuit voltage (V_{OC}) and PCE of dye sensitized solar cells can be significantly enhanced. In order to retain the use of TBP as an additive in the HTL and eliminate the corrosion effect, montmorillonite (MMT) with an intercalated structure was introduced as a buffer layer in PSCs to retard the TBP corrosion of perovskite. The protection of MMT was determined by the absorption of a film with a threefold greater concentration of TBP in the HTM (Fig. 7a). The absorption intensity was enhanced by adding the MMT buffer layer. IR and XRD results showed that the MMT could interact with TBP through hydrogen bonds in its intercalated structure. UV-vis results showed that the MMT could protect the perovskite from corrosion by TBP. With the addition of MMT, the corresponding efficiency of the device shown in Fig. 7b was improved by 32.2%, and an overall efficiency of 11.9% was obtained under AM 1.5 sunlight. The increase in J_{SC} was attributed to the absorption enhancement evidenced by UV-vis measurement, owing to the suppressed corrosion. The improved V_{OC} and especially FF values further indicated the presence of limited electron recombination processes. This was evidenced by the electrochemical impedance spectra (EIS), in which an increase in the interface resistance in the dark was observed, and the dark current curves, in which the dark current declined with increasing voltage. This study presents an applicable strategy for interfacial engineering in PSCs.

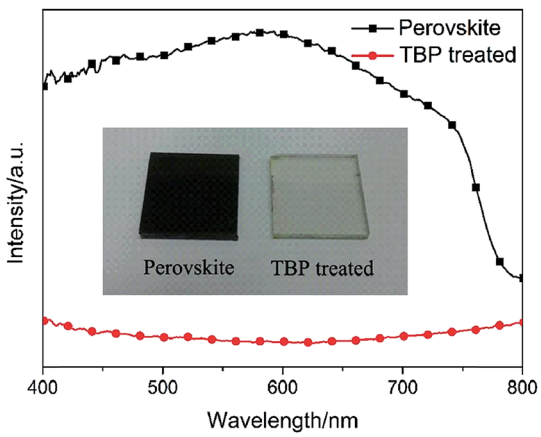

Fig. 6 UV-vis spectra of TiO_2/perovskite film and TBP treated film. The inset shows a photograph of the films before and after TBP treatment. Reproduced from ref. 37 with permission from The Royal Society of Chemistry.

Zhu and co-workers found that the perovskite was sensitive to NH_3.[42] When passing through the opening of a bottle containing 3% NH_3 solution, the perovskite film immediately turned colorless (Fig. 8a–c). UV-vis absorption spectra (Fig. 8d) verified the immediate decrease in the absorption of $CH_3NH_3PbI_3$ in the presence of NH_3 gas. The photoresponse of $CH_3NH_3PbI_3$ film at 660 nm (Fig. 8e) shows that the transmitted light intensity increased very quickly (<1 s) after the introduction of NH_3, and also decreased quickly (1–2 s) after NH_3 was removed. An unknown XRD peak at about 11.6° arose after the NH_3 treatment. This characteristic peak cannot be assigned to either $CH_3NH_3PbI_3$ or PbI_2. Further studies are required to understand how the crystal structure of $CH_3NH_3PbI_3$ evolves in the presence of NH_3, and how the crystal structure of NH_3-treated $CH_3NH_3PbI_3$ changes upon the removal of NH_3 from the environment.

In summary, additives in the HTM, such as TBP, are dangerous to the perovskite. During the solvent evaporation process, DMF residue can also degrade the perovskite. Moreover, PSCs are very sensitive to impurities in the solvent and solute. The slight amount of water adsorbed in air conditions will lead to the irreversible decomposition of perovskite. As a result, we should develop substitutes for TBP and pay attention to the environment for spin-coating during the film fabrication process. Novel modification materials at the interface between the photoanode and perovskite may be another possible protection route.

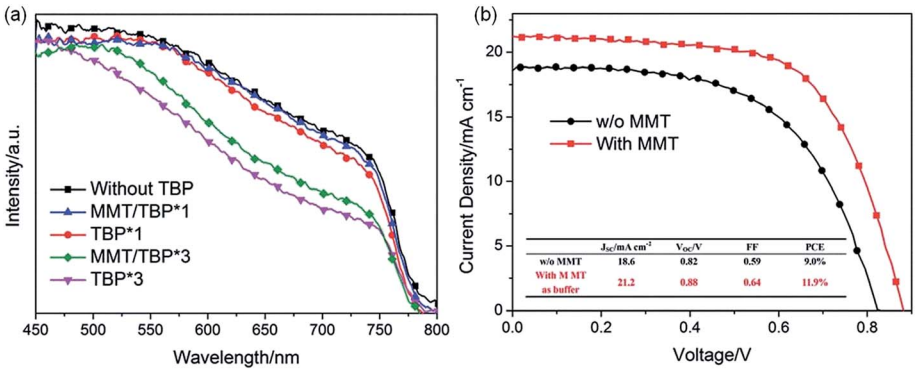

Fig. 7 (a) UV-vis absorption of TiO_2/perovskite films without TBP treatment (black line); without (red line) and with (blue line) MMT modification capped with an HTL including a certain concentration of TBP (TBP*1); without (green) and with (pink) MMT modification corroded by a concentration of TBP three times greater than that of TBP*1. (b) The *J*–*V* characteristics of devices without MMT addition (black line) and with MMT addition (red line) to the HTL; the inset shows the parameters of the cells. Adapted from ref. 37 with permission from The Royal Society of Chemistry.

2.4 The chemical stability of PSCs in thermal conditions

In a typical solution process for perovskite film fabrication, annealing is necessary for the formation of the perovskite crystal structure. However, the perovskite itself, and other components, may be susceptible to damage during thermal annealing. Here, we summarize the effects of thermal treatment on the crystal structure, the decomposition of perovskite, and the thermal stability of the HTM layers.

2.4.1 Crystal structure stability of perovskite. Crystal and phase transition is a key physical–chemical conversion process in PSCs. The crystalline phase of organic–inorganic hybrid perovskite can change *via* its own properties and due to environmental conditions, such as temperature, pressure, which directly affect the stability of PSCs. This section will cover the stability of PSCs under thermal conditions, as well as the relationship of the crystal structure with pressure, to provide a comprehensive understanding of the crystal structure of perovskite.

In ABX_3 (A = alkali; B = Ge, Sn, Pb and X = halide) structure, A is commonly a large cation coordinated to 12X anions, and B

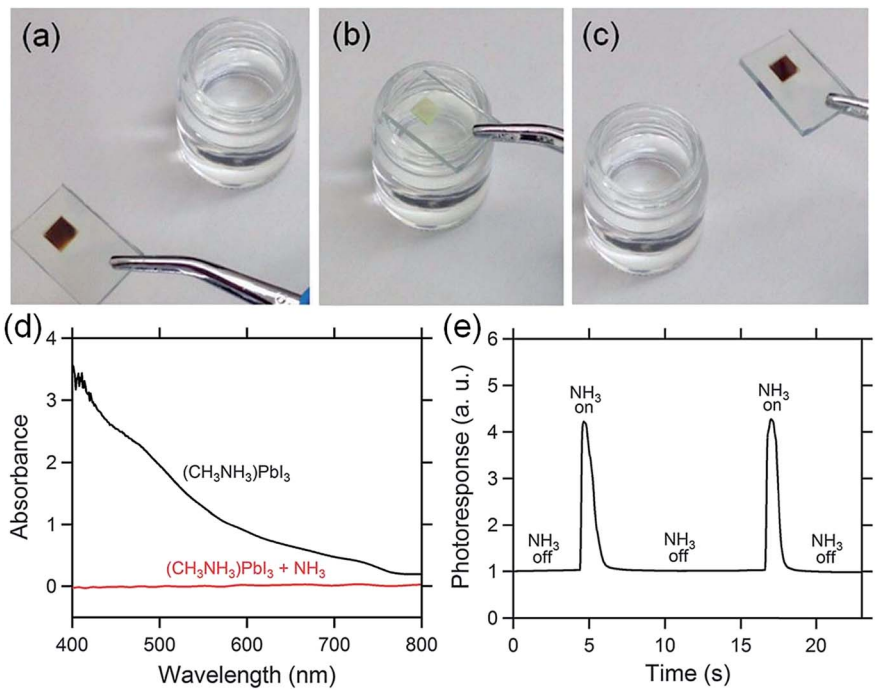

Fig. 8 The sequence (a) to (c) of the color change of a $CH_3NH_3PbI_3$ film (deposited on a mesoporous TiO_2 film on FTO) passing through the top opening of a 3% NH_3 solution bottle. (d) UV-vis absorption spectra of the film in the absence and presence of NH_3 gas. (e) Photoresponse of $CH_3NH_3PbI_3$ film at 660 nm, measured using a silicon detector, in response to the introduction and removal of NH_3 gas. Adapted from ref. 42 with permission from The Royal Society of Chemistry.

is a smaller metal bonded to six X anions, forming corner-sharing BX_6 octahedra in a three-dimensional framework.[24] To study the stability of ABX_3 perovskite, Goldschmidt (1927) proposed a tolerance factor (t), which is defined as:

$$t = \frac{r_A + r_X}{\sqrt{2}(r_B + r_X)} \quad (4)$$

where r_A, r_B and r_X are the ionic radii for the ions in the A, B and X sites, respectively.

To form a stable perovskite structure, the size of the ionic radius is restrained by the tolerance factor. For a perfectly packed cubic perovskite structure, $t = 1$. Empirically, for the most stable perovskite, t corresponds to values between 0.8 and 1,[43,44] and an increase in t generally leads to an increase in symmetry, with an expected reduction in the electronic band gap.[45] Based on the prototype perovskite $CH_3NH_3PbI_3$ in solar cells, various components, such as Cs^+,[46] $CH_3CH_2NH_3^+$,[47] $HN{=}CHNH_3^+$,[45,48–51] Sn^{2+},[52–54] Cl^-,[7,54–56] Br^-,[18,57,58] and BF_4^-,[59] have been introduced to modulate the crystal structure and the band gap.

In addition to the ionic radius, phase transition in response to temperature and pressure is also a significant aspect affecting the structural stability. Weber and co-workers reported the temperature-dependent structure of methylammonium trihalide perovskite $CH_3NH_3PbX_3$ (X = Cl, Br, I).[60] As tabulated in Table 1, the symmetry increases with temperature. It is also worth noting that at room temperature, $CH_3NH_3PbI_3$ forms a tetragonal structure, whereas $CH_3NH_3PbBr_3$ and $CH_3NH_3PbCl_3$ form cubic structures, in line with the law that symmetry increases with t. Baikie and co-workers gave a detailed description of the preparation, structural characterization and physical characteristics of typical $CH_3NH_3PbI_3$.[24] With powder X-ray diffraction and differential scanning calorimetry (DSC), they noticed that at a higher temperature (nearly 56 °C), the tetragonal perovskite would totally transform into the cubic structure. A transient intermediate phase was indicated by the asymmetric DSC peaks, although it could not be detected by powder X-ray diffraction.

Moreover, Swainson and co-workers found a phase transition of $CH_3NH_3PbBr_3$ just below 1 GPa and amorphized around 2.8 GPa, without the process of cations undergoing long-range orientational ordering.[61] The volume reduction under compression was attributed to the tilting of the $PbBr_6$ octahedra. Suga and co-workers also gave the pressure–temperature phase relations of $CH_3NH_3PbX_3$ (X = Cl, Br, I) crystals in the range between 0.1 Pa and 200 MPa in detail.[62]

The symmetry variation caused by octahedra tilting corresponding to both temperature and pressure affects the electronic and optical properties of perovskite,[44] and therefore influences the photovoltaic performance of PSC devices. However, few reports focus on the effects of phase transition on device performance, and this type of work would be significant for the commercial applications of PSCs.

2.4.2 Thermal decomposition of perovskite. For PSCs working under sun illumination, the temperature of the solar cells seems to be greater than the transition temperature for $CH_3NH_3PbI_3$, thus whether the phase transition can affect the performance of solar cells still needs to be verified. Grätzel and co-workers studied the thermal behavior of the perovskite and

Table 1 Temperature-dependent structural data of $MAPbX_3$ (X = Cl, Br, I). Adapted from ref. 60, Copyright© 1987 American Institute of Physics

Phase	Temperature (K)	Crystal system	Space group	Lattice (pm)	Volume (10^6 pm^3)
$CH_3NH_3PbCl_3$					
α	>178.8	Cubic	*Pm*3*m*	$a = 567.5$	182.8
β	172.9–178.9	Tetragonal	*P*4/*mmm*	$a = 565.5$ $c = 563.0$	180.1
γ	<172.9	Orthorhombic	$P222_1$	$a = 567.3$ $b = 562.8$ $c = 1118.2$	357.0
$CH_3NH_3PbBr_3$					
α	>236.9	Cubic	*Pm*3*m*	$a = 590.1(1)$	206.3 (260 K)
β	155.1–236.9	Tetragonal	*I*4/*mcm*	$a = 832.2(2)$ $c = 1183.2(7)$	819.4
γ	149.5–155.1	Tetragonal	*P*4/*mmm*	$a = 589.4(2)$ $c = 586.1(2)$	
δ	<144.5	Orthorhombic	$Pna2_1$	$a = 797.9(1)$ $b = 858.0(2)$ $c = 1184.9(2)$	811.1
$CH_3NH_3PbI_3$					
α	>327.4	Cubic	*Pm*3*m*	$a = 632.85(4)$	253.5
β	162.2–327.4	Tetragonal	*I*4/*mcm*	$a = 885.5(6)$ $c = 1265.9(8)$	992.6
γ	<162.2	Orthorhombic	$Pna2_1$	$a = 886.1(2)$ $b = 858.1(2)$ $c = 1262.0(3)$	959.5

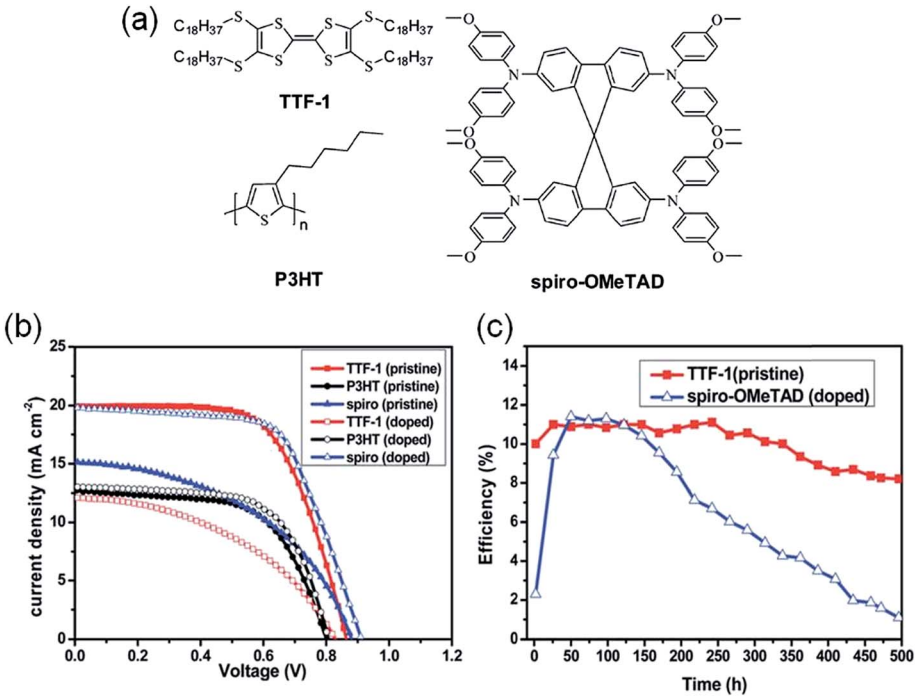

Fig. 9 (a) Molecular structure of TTF-1, P3HT, and spiro-OMeTAD. (b) Current–voltage curves of PSCs based on TTF-1, P3HT and spiro-OMeTAD in the pristine form or doped with Li-TFSI and TBP. (c) Stability test at room temperature with a humidity of 40% and measured under illumination at AM 1.5 G. Adapted from ref. 67 with permission from The Royal Society of Chemistry.

its individual components.[63] They found that the deposition method could affect the phase transition process from the tetragonal to the cubic phase. In contrast to the PbI_2 precursor based method, the phase transition process was not found in the $PbCl_2$ based case. It was believed that these subtle differences in the formation process would ultimately influence the photovoltaic performance and stability of the devices. In their paper, Grätzel and co-workers also point out that during the decomposition process of perovskite, the loss of CH_3NH_2 lags behind the HI due to its tighter incorporation in the perovskite matrix. This behavior might also affect the long-term stability of the perovskite. Pisoni and co-workers reported the thermal conductive properties of $CH_3NH_3PbI_3$.[64] Their research showed that $CH_3NH_3PbI_3$ had a very low thermal conductivity for both large single crystals and the polycrystalline form. This meant that the light-deposited heat inside the perovskite itself could not spread out quickly, which caused mechanical stress and limited the lifetime of the photovoltaic devices.

Recently, Snaith and co-workers demonstrated an approach to effectively retard thermal degradation by replacing the organic hole transport material with polymer-functionalized single-walled carbon nanotubes (SWNTs) embedded in an insulating polymer matrix.[65] In addition, the resistance to moisture was also remarkably enhanced.

2.4.3 Thermal stability of HTM layers. Apart from the thermal stability of perovskite itself, other layers in a photovoltaic device can also have a great influence on its long-term performance. Compared with the organic materials used in the device, the inorganic blocking layer and scaffold layer seem to be sufficiently stable for practical application. Here, we mainly focus on the spiro-OMeTAD based hole transport layer because it has been so widely used and studied thoroughly. Wu and co-workers recently gave a very detailed report on the impact of annealing on spiro-OMeTAD and the corresponding devices.[66] They found that, after annealing, the crystallization and oxidation of spiro-OMeTAD was enhanced as expected, which was beneficial for the hole transfer and transport. As a result, a higher short-circuit current was obtained. However, due to the transfer of Li-TFSI to the TiO_2 surface and the evaporation of 4-*tert*-butylpyridine, the Fermi level of TiO_2 shifted down. This led to a considerably lower V_{OC} and fill factor, and finally to decreased power conversion efficiency. The same results were also observed in our lab. Though the annealing temperature (85 °C) was considerably lower than the glass transition temperature of spiro-OMeTAD (around 125 °C), the performance of the solar cells greatly decreased after a long period of annealing.

Other, more stable hole transport materials have been reported. Han and co-workers introduced a tetrathiafulvalene derivative (TTF-1) into PSCs without the use of p-type dopants.[67] The chemical structures of TTF-1, P3HT, and spiro-OMeTAD are shown in Fig. 9a. The cells employing TTF-1 as the hole transport layer achieved a PCE of 11.03%, comparable to that of a device with p-type doped spiro-OMeTAD (11.4%), as illustrated in Fig. 9b. Moreover, the stability of the device is considerably better than that of the spiro-OMeTAD based device (Fig. 9c). The stability test was conducted at room temperature with a humidity of about 40%. The improved stability was attributed to the avoidance of the use of deliquescent additives and hydrophobic alkyl chains in TTF-1.

Another choice to resolve the issue of instability of the spiro-OMeTAD based hole transport layer is to remove it from the device. Meng and co-workers reported no-HTL-structured perovskite devices, and 10.5% power conversion efficiency was achieved.[68] Han and co-workers used printable carbon as the back contact and fabricated hole-conductor-free PSCs. After exposure to full AM 1.5 simulated sunlight over 1008 h in ambient conditions without sealing, the final PCE of the device even increased slightly.[69]

3. Conclusions and outlook

In summary, research on the chemical stability of PSCs under different conditions has attracted increasing attention, but a basic understanding of the chemical stability, especially the thermal stability, still requires further exploration efforts. In order to modulate the stability of PSCs, many factors should be taken into consideration for their systematic engineering, including the composition and crystal structure design of the perovskite, the preparation of the HTM layer and electrode materials, the thin film fabrication method, interfacial engineering, encapsulation methods (multilayer encapsulation or helmet encapsulation), and the module technology. Additionally, studies on the stability of PSCs, and how to improve the stability of the devices under different conditions, are insufficient. Currently, in order to address these key theoretical issues and technical tasks, some groups have started to investigate the stability of PSCs. The mechanism of degradation should also be studied in order to predict the behavior of perovskite in different conditions. To improve the stability of perovskites, the degradation processes of all types of perovskites, such as $CH_3NH_3PbBr_3$, $CH_3NH_3PbCl_3$ or $CH_3NH_3SnI_3$, should be studied in much greater detail. By combining resistivity to specific conditions with the strong absorption properties and carrier mobility of PSCs, stable solar cells with high performance are realizable in the near future. The fabrication process of perovskite solar cells, including the environment during film formation, the exact role of the additives, and the optimal device architecture, should all be carefully considered to determine a standard procedure for the manufacturing process. This would be promising to obtain new breakthroughs in the stability of PSCs and establish foundations for the commercialization and outdoor applications of PSCs.

Acknowledgements

This work was supported by the National Natural Science Foundation of China under Grant no. 51273104 and the National Key Basic Research and Development Program of China under Grant no. 2009CB930602.

References

1 N. G. Park, *J. Phys. Chem. Lett.*, 2013, **4**, 2423–2429.
2 G. Xing, N. Mathews, S. Sun, S. S. Lim, Y. M. Lam, M. Grätzel, S. Mhaisalkar and T. C. Sum, *Science*, 2013, **342**, 344–347.
3 M. Grätzel, *Nat. Mater.*, 2014, **13**, 838–842.
4 *Science*, 2013, **342**, 1438–1439.
5 A. Kojima, K. Teshima, Y. Shirai and T. Miyasaka, *J. Am. Chem. Soc.*, 2009, **131**, 6050–6051.
6 H. S. Kim, C. R. Lee, J. H. Im, K. B. Lee, T. Moehl, A. Marchioro, S. J. Moon, R. Humphry-Baker, J. H. Yum, J. E. Moser, M. Grätzel and N. G. Park, *Sci. Rep.*, 2012, **2**, 591.
7 M. M. Lee, J. Teuscher, T. Miyasaka, T. N. Murakami and H. J. Snaith, *Science*, 2012, **338**, 643–647.
8 J. Burschka, N. Pellet, S.-J. Moon, R. Humphry-Baker, P. Gao, M. K. Nazeeruddin and M. Grätzel, *Nature*, 2013, **499**, 316–319.
9 H. Zhou, Q. Chen, G. Li, S. Luo, T.-b. Song, H.-S. Duan, Z. Hong, J. You, Y. Liu and Y. Yang, *Science*, 2014, **345**, 542–546.
10 M. Liu, M. B. Johnston and H. J. Snaith, *Nature*, 2013, **501**, 395–398.
11 L. Etgar, P. Gao, Z. Xue, Q. Peng, A. K. Chandiran, B. Liu, M. K. Nazeeruddin and M. Grätzel, *J. Am. Chem. Soc.*, 2012, **134**, 17396–17399.
12 W. A. Laban and L. Etgar, *Energy Environ. Sci.*, 2013, **6**, 3249–3253.
13 Q. Chen, H. Zhou, Z. Hong, S. Luo, H.-S. Duan, H.-H. Wang, Y. Liu, G. Li and Y. Yang, *J. Am. Chem. Soc.*, 2013, **136**, 622–625.
14 http://www.nrel.gov/ncpv/images/efficiency_chart.jpg.
15 H. J. Snaith, *J. Phys. Chem. Lett.*, 2013, **4**, 3623–3630.
16 H. S. Kim, S. H. Im and N. G. Park, *J. Phys. Chem. C*, 2014, **118**, 5615–5625.
17 M. He, D. Zheng, M. Wang, C. Lin and Z. Lin, *J. Mater. Chem. A*, 2014, **2**, 5994–6003.
18 J. H. Noh, S. H. Im, J. H. Heo, T. N. Mandal and S. I. Seok, *Nano Lett.*, 2013, **13**, 1764–1769.
19 G. Niu, W. Li, F. Meng, L. Wang, H. Dong and Y. Qiu, *J. Mater. Chem. A*, 2014, **2**, 705–710.
20 B. Ma, R. Gao, L. Wang, F. Luo, C. Zhan, J. Li and Y. Qiu, *J. Photochem. Photobiol., A*, 2009, **202**, 33–38.
21 W. Li, J. Li, L. Wang, G. Niu, R. Gao and Y. Qiu, *J. Mater. Chem. A*, 2013, **1**, 11735–11740.
22 J. M. Frost, K. T. Butler, F. Brivio, C. H. Hendon, M. van Schilfgaarde and A. Walsh, *Nano Lett.*, 2014, **14**, 2584–2590.
23 Z. Cheng and J. Lin, *CrystEngComm*, 2010, **12**, 2646–2662.
24 T. Baikie, Y. Fang, J. M. Kadro, M. Schreyer, F. Wei, S. G. Mhaisalkar, M. Grätzel and T. J. White, *J. Mater. Chem. A*, 2013, **1**, 5628–5641.
25 I. C. Smith, E. T. Hoke, D. Solis-Ibarra, M. D. McGehee and H. I. Karunadasa, *Angew. Chem., Int. Ed.*, 2014, **53**, 11232–11235.
26 E. Muljarov, S. Tikhodeev, N. Gippius and T. Ishihara, *Phys. Rev. B: Condens. Matter Mater. Phys.*, 1995, **51**, 14370–14378.
27 T. Ishihara, *J. Lumin.*, 1994, **60**, 269–274.
28 M. D. Kempe, A. A. Dameron and M. O. Reese, *Prog. Photovoltaics*, 2014, **22**, 1159–1171.
29 A. Fujishima, T. N. Rao and D. A. Tryk, *J. Photochem. Photobiol., C*, 2000, **1**, 1–21.
30 S. Ito, S. Tanaka, K. Manabe and H. Nishino, *J. Phys. Chem. C*, 2014, **118**, 16995–17000.

31 R. J. Ouellette, *Organic Chemistry: A Brief Introduction*, Prentice Hall, Upper Saddle River, NJ, 2nd edn, 1997.
32 T. Leijtens, G. E. Eperon, S. Pathak, A. Abate, M. M. Lee and H. J. Snaith, *Nat. Commun.*, 2013, **4**, 2885.
33 S. K. Pathak, A. Abate, T. Leijtens, D. J. Hollman, J. Teuscher, L. Pazos, P. Docampo, U. Steiner and H. J. Snaith, *Adv. Energy Mater.*, 2014, **4**, 1301667.
34 K. Schwanitz, U. Weiler, R. Hunger, T. Mayer and W. Jaegermann, *J. Phys. Chem. C*, 2007, **111**, 849–854.
35 N. Chander, A. Khan, P. Chandrasekhar, E. Thouti, S. K. Swami, V. Dutta and V. K. Komarala, *Appl. Phys. Lett.*, 2014, **105**, 033904.
36 P. Strange, A. Svane, W. Temmerman, Z. Szotek and H. Winter, *Nature*, 1999, **399**, 756–758.
37 W. Li, H. Dong, L. Wang, N. Li, X. Guo, J. Li and Y. Qiu, *J. Mater. Chem. A*, 2014, **2**, 13587–13592.
38 H. Zhang, Y. Shi, F. Yan, L. Wang, K. Wang, Y. Xing, Q. Dong and T. Ma, *Chem. Commun.*, 2014, **50**, 5020–5022.
39 J. H. Heo and S. H. Im, *Phys. Status Solidi RRL*, 2014, **8**, 816–821.
40 H. J. Snaith, A. Abate, J. M. Ball, G. E. Eperon, T. Leijtens, N. K. Noel, S. D. Stranks, J. T.-W. Wang, K. Wojciechowski and W. Zhang, *J. Phys. Chem. Lett.*, 2014, **5**, 1511–1515.
41 A. Dualeh, T. Moehl, N. Tétreault, J. Teuscher, P. Gao, M. K. Nazeeruddin and M. Grätzel, *ACS Nano*, 2013, **8**, 362–373.
42 Y. Zhao and K. Zhu, *Chem. Commun.*, 2014, **50**, 1605–1607.
43 D. B. Mitzi, *Prog. Inorg. Chem.*, 2007, **48**, 1–121.
44 A. Amat, E. Mosconi, E. Ronca, C. Quarti, P. Umari, M. K. Nazeeruddin, M. Grätzel and F. De Angelis, *Nano Lett.*, 2014, **14**, 3608–3616.
45 T. M. Koh, K. Fu, Y. Fang, S. Chen, T. C. Sum, N. Mathews, S. G. Mhaisalkar, P. P. Boix and T. Baikie, *J. Phys. Chem. C*, 2014, **118**, 16458–16462.
46 H. Choi, J. Jeong, H.-B. Kim, S. Kim, B. Walker, G.-H. Kim and J. Y. Kim, *Nano Energy*, 2014, **7**, 80–85.
47 J. H. Im, J. Chung, S. J. Kim and N. G. Park, *Nanoscale Res. Lett.*, 2012, **7**, 353.
48 J. W. Lee, D. J. Seol, A. N. Cho and N. G. Park, *Adv. Mater.*, 2014, **26**, 4991–4998.
49 N. Pellet, P. Gao, G. Gregori, T. Y. Yang, M. K. Nazeeruddin, J. Maier and M. Grätzel, *Angew. Chem., Int. Ed.*, 2014, **53**, 3151–3157.
50 G. E. Eperon, S. D. Stranks, C. Menelaou, M. B. Johnston, L. M. Herz and H. J. Snaith, *Energy Environ. Sci.*, 2014, **7**, 982–988.
51 S. Pang, H. Hu, J. Zhang, S. Lv, Y. Yu, F. Wei, T. Qin, H. Xu, Z. Liu and G. Cui, *Chem. Mater.*, 2014, **26**, 1485–1491.
52 C. C. Stoumpos, C. D. Malliakas and M. G. Kanatzidis, *Inorg. Chem.*, 2013, **52**, 9019–9038.
53 Y. Ogomi, A. Morita, S. Tsukamoto, T. Saitho, N. Fujikawa, Q. Shen, T. Toyoda, K. Yoshino, S. S. Pandey and T. Ma, *J. Phys. Chem. Lett.*, 2014, **5**, 1004–1011.
54 F. Hao, C. C. Stoumpos, D. H. Cao, R. P. Chang and M. G. Kanatzidis, *Nat. Photon.*, 2014, **8**, 489–494.
55 B. Suarez, V. Gonzalez-Pedro, T. S. Ripolles, R. S. Sánchez, L. A. Otero and I. Mora-Sero, *J. Phys. Chem. Lett.*, 2014, **5**, 1628–1635.
56 S. Colella, E. Mosconi, P. Fedeli, A. Listorti, F. Gazza, F. Orlandi, P. Ferro, T. Besagni, A. Rizzo and G. Calestani, *Chem. Mater.*, 2013, **25**, 4613–4618.
57 E. Edri, S. Kirmayer, M. Kulbak, G. Hodes and D. Cahen, *J. Phys. Chem. Lett.*, 2014, **5**, 429–433.
58 E. Edri, S. Kirmayer, D. Cahen and G. Hodes, *J. Phys. Chem. Lett.*, 2013, **4**, 897–902.
59 S. Nagane, U. Bansode, O. Game, S. Chhatre and S. Ogale, *Chem. Commun.*, 2014, **50**, 9741–9744.
60 A. Poglitsch and D. Weber, *J. Chem. Phys.*, 1987, **87**, 6373–6378.
61 I. Swainson, M. Tucker, D. Wilson, B. Winkler and V. Milman, *Chem. Mater.*, 2007, **19**, 2401–2405.
62 N. Onodayamamuro, O. Yamamuro, T. Matsuo and H. Suga, *J. Phys. Chem. Solids*, 1992, **53**, 277–281.
63 A. Dualeh, P. Gao, S. I. Seok, M. K. Nazeeruddin and M. Grätzel, *Chem. Mater.*, 2014, **26**, 6160–6164.
64 A. Pisoni, J. Jacimovic, O. S. Barišić, M. Spina, R. Gaál, L. Forró and E. Horváth, *J. Phys. Chem. Lett.*, 2014, **5**, 2488–2492.
65 S. N. Habisreutinger, T. Leijtens, G. E. Eperon, S. D. Stranks, R. J. Nicholas and H. J. Snaith, *Nano Lett.*, 2014, **14**, 5561–5568.
66 Y. Fang, X. Wang, Q. Wang, J. Huang and T. Wu, *Phys. Status Solidi A*, 2014, **211**, 2809–2816.
67 J. Liu, Y. Wu, C. Qin, X. Yang, T. Yasuda, A. Islam, K. Zhang, W. Peng, W. Chen and L. Han, *Energy Environ. Sci.*, 2014, **7**, 2963–2967.
68 J. Shi, J. Dong, S. Lv, Y. Xu, L. Zhu, J. Xiao, X. Xu, H. Wu, D. Li, Y. Luo and Q. Meng, *Appl. Phys. Lett.*, 2014, **104**, 063901.
69 A. Mei, X. Li, L. Liu, Z. Ku, T. Liu, Y. Rong, M. Xu, M. Hu, J. Chen, Y. Yang, M. Grätzel and H. Han, *Science*, 2014, **345**, 295–298.

